Chemical Engineering Journal 162 (2010) 528–536

Contents lists available at ScienceDirect

Chemical Engineering Journal

journal homepage: www.elsevier.com/locate/cej

The weaknesses of a k–ε model compared to a large-eddy simulation for the prediction of UV dose distributions and disinfection

B.A. Wols [a,b,*], W.S.J. Uijttewaal [b], J.A.M.H. Hofman [a,b], L.C. Rietveld [b], J.C. van Dijk [b]

[a] KWR Research Institute, 3433 PE Nieuwegein, The Netherlands
[b] Delft University of Technology, 2600 GA Delft, The Netherlands

ARTICLE INFO

Article history:
Received 18 February 2010
Received in revised form 26 May 2010
Accepted 26 May 2010

Keywords:
CFD
Turbulence modelling
Large-eddy simulation
k–ε model
Dose distribution
UV disinfection

ABSTRACT

CFD modelling has proven to be a powerful tool for the design of UV reactors. However, the validation of the hydraulics predicted by the CFD model remains a point of attention. Using standard turbulence models such as the k–ε model, the CFD model often wrongly predicts local flow features around a UV lamp. Therefore, more advanced modelling approaches such as the LES model were considered. The modelling approaches were explored for a single cross-flow UV lamp. It is shown by means of comparison with experimental data that the LES model predicts the flow around a UV lamp more precisely than the k–ε model. The impact of differences in resolved velocity fields on the predicted disinfection was also investigated. Depending on the local geometry (presence and positioning of baffles) the disinfection results were completely different for the different modelling approaches.

© 2010 Elsevier B.V. All rights reserved.

1. Introduction

Disinfection by UV light is increasingly applied in water treatment systems. The inactivation of microorganisms depends on the amount of UV light a microorganism receives during its path through the UV installation, which is known as the UV dose. This UV dose is mainly determined by the hydraulics inside the system. Spatial differences in UV irradiation as well as spatial and temporal variations in water velocities and (turbulent) mixing properties result in a particular distribution of UV doses. This distribution forms a measure for the disinfection efficacy of a UV system. For a proper prediction of the performance of a UV system, sophisticated modelling techniques are required to capture the complex hydraulic processes. Computational fluid dynamics (CFD) models are therefore often used to predict the disinfection efficacy and optimize UV systems [1–6]. The simulation of UV systems involves the prediction of flow fields, UV irradiation fields and microbial inactivation. The movements of individual particles are calculated using the resolved flow fields, from which the UV dose distribution is determined. The most challenging part of the simulation is to predict the flow fields correctly. The complex turbulent flows require a detailed numerical modelling to resolve all the relevant turbulent scales, which results in long and expensive computations. Simplified turbulence models (such as the k–ε model) are therefore used in practice to reduce the computational time. As a consequence, the flow fields often are predicted incorrectly, especially around complex geometries [8]. A system with UV lamps placed perpendicular to the flow direction is such a complex geometry, where the lamp forms an obstacle in the flow that produces a non-trivial turbulent flow pattern.

Using a large-eddy simulation (LES) that resolves most of the turbulent eddies, instead of using a Reynolds-averaged Navier–Stokes (RANS) approach, the flow fields are predicted more precisely [7,8]. Resolving the unsteady turbulent motions results in a different flow pattern than predicted by the k–ε model. As a result, it is expected that the transport of particles also differs largely for the k–ε model compared to the LES model. Consequently, predictions for the disinfection will be different. From the literature, limited information is available about the effect of more detailed flow computation on the actual disinfection prediction: for example, how the predicted size of the wake influences the disinfection remains unclear. The wake behind the lamp is under predicted by a CFD model using the RANS approach with a standard k–ε turbulence model [8,9]. Liu et al. [9] investigated several turbulence models in combination with the RANS equations. They also found an under prediction of the wake size by the standard k–ε model compared to measurements. Some other turbulence models showed a similar behaviour; the k–ω model did show a better prediction of the wake size, but the far wake region was predicted wrongly. The Reynolds stress model showed the best results, probably because it accounts for the anisotropic viscosity. Although the

* Corresponding author at: KWR Watercycle Research Institute, 3433 PE Nieuwegein, The Netherlands.
E-mail addresses: b.a.wols@tudelft.nl, bas.wols@kwrwater.nl (B.A. Wols).

1385-8947/$ – see front matter © 2010 Elsevier B.V. All rights reserved.
doi:10.1016/j.cej.2010.05.055

differences in wake sizes between the different turbulence models were significant, the differences in disinfection levels were small (within 5%). Some authors included the dynamic behaviour of the vortex shedding by means of an unsteady k–ε turbulence model and found only small differences with the stationary approach [10,11]. However, they still used the RANS approach, so not all the relevant turbulent length scales that influenced the wake formation were resolved. Therefore, we will use the LES model which represent the physical processes more precisely and compare it to the RANS approach with a standard k–ε turbulence model. An assessment is made of the effect of both modelling approaches (LES model and k–ε model) on the residence time distributions, dose distributions and disinfection efficacy for some simplified UV systems. UV systems were not yet assessed by the LES model. A cross-flow system with a single lamp is considered here, which focuses on the detailed flow field around a single UV lamp. In addition, configurations with baffles in the neighbourhood of a single lamp are considered. By considering a small part of a full-scale UV reactor in detail, such as the flow field around a single UV lamp, the reliability of different CFD models will be further clarified. The aim is to assess the accuracy of the available modelling techniques with respect to the flow fields, and how the inaccuracies in the calculated flow field influence the disinfection prediction. Because of the large difference in wake prediction behind the lamp by both modelling approaches, the sensitivity of the wake size to the disinfection will be clarified as well.

2. Materials and methods

2.1. Modelling approaches

Two types of modelling approaches were considered here: a Reynolds-averaged Navier–Stokes equation (RANS) with a standard k–ε turbulence model, referred to as k–ε model, and a large-eddy simulation, referred to as LES model. The standard k–ε model is most often used for engineering applications. The time-varying turbulent motions are captured in the averaged variables k and ε (Appendix A). Results can be obtained at acceptable computational costs (e.g., within 1 or 2 days). These types of models are therefore most often used for the design or optimization of large-scale installations, such as UV reactors. A large-eddy simulation [12] has much higher computational costs (e.g., around 2 weeks on multiple CPUs), but results in more detailed and accurate results, because the time-varying turbulent motions are resolved. A LES is often used as a research tool for a better understanding of local transport mechanisms. Knowledge on the local and instantaneous concentrations is particularly important for simulations involving chemical or microbiological reactions, because the localized areas of high concentration may result in a higher reaction rate than calculated by an averaged concentration from the RANS approach. The choice for a k–ε model or a LES is a trade-off between accuracy and computational speed. Both methods will be used here and the differences between these methods for the flow around a single UV lamp will be explored.

Furthermore, the trajectories of individual particles were calculated. Fluctuations of the particle motions induced by the turbulent motions model the mixing processes precisely. These particles are assumed to represent microorganisms (size of 1–5 μm) that are smaller than the Kolmogorov microscales ($\sim 10^{-4}$–10^{-3} m). As a result, these particles move entirely with the fluid [18]. Since the LES model resolves the time-varying velocity fields, the particle motions – which are motions induced by advection – are solved accurately. The particle movement in the LES model only consists of an advection displacement induced by the fluctuating velocity field. Since the LES model resolves the most energy containing turbulent eddies, which are eddies at a scale of the mesh size and larger, the advection displacement dominates over the viscosity displacement, which is therefore neglected. For the k–ε model, the particle movements consist of an advection displacement induced by the calculated steady velocity field and a random displacement induced by the turbulent viscosity. The turbulent viscosity coefficient is determined from the variables k and ε (Appendix A). However, by introducing an artificial random displacement [19] obtained from a viscosity coefficient that mimics the advective transport of the turbulent motions, the calculated particle trajectories may be inaccurate. This is illustrated in Fig. A1 of the supplementary appendix for the flow around a cylinder. The LES model calculates time-varying velocity fields, which are continuously changing due to the turbulent motions; a snapshot is shown in the upper panel of the figure. The k–ε model only calculates a stationary mean velocity field. This particular velocity field will not occur in nature, in fact, it will always differ significantly from the instantaneous velocity field in reality. The particle trajectories plotted in Fig. A1 of the supplementary appendix underline these differences: the large vortices downstream of the cylinder calculated by the LES model move particles upward and downward over large distances, which does not occur for the particles in the k–ε model.

Both modelling approaches were used in different computational codes:

- For the k–ε model, a commercial available finite-element package, COMSOL v3.5, was used. The flow domain is discretized with tetrahedrons.
- For the LES model, a finite-difference model [13] was used. The equations were solved on a structured Cartesian grid using finite-differences. A staggered grid was used, where the scalars (pressure, eddy viscosity) were solved in the middle of the volume and the vectors (velocities) were solved at the boundaries.

2.2. Validation of models by means of velocity fields

The velocity fields calculated by the CFD models were validated by laser Doppler anemometry (LDA) measurements, a non-intrusive technique to measure the velocity at a single point in the flow domain. The measurements were conducted in a long square flume (water height = 0.4 m, width = 0.4 m, length = 13 m). A cylinder was placed in the middle of the flume, which resulted in a comparable situation as the reference configuration. The diameter of the cylinder (D = 5 cm) was approximately equal to the size of the quartz sleeve in a bench-scale UV reactor [20]. The instantaneous velocities were measured during 3 min at different positions in the flume, from which the mean velocities and Reynolds stresses were determined. A CFD model was constructed using the same geometry as for the experiment. The results of the streamwise velocities for the k–ε model as well as the LES model are shown in Fig. 1. The flow fields were better described using the LES model than the k–ε model. The k–ε model had under predicted the wake region downstream of the cylinder: the velocities were still positive, whereas a clear reversed flow occurred in the measurements. Outside the wake region and further downstream of the cylinder (at x = 15 cm), the k–ε model predicted velocities in correspondence with the measurements. The velocities determined by the LES model were in good agreement with the measurements.

Both modelling approaches were also compared to the flow fields measured in a bench-scale UV reactor [20], Fig. S1 of the supplementary information. Again the flow fields were better described by the LES model than the k–ε model, especially downstream of the lamps (cross-section 3 and 4). The wake region is largely under predicted by the k–ε model. More details about the measurements and validation of the CFD models are provided by Wols et al. [8]. This paper focuses on how these differences in veloc-

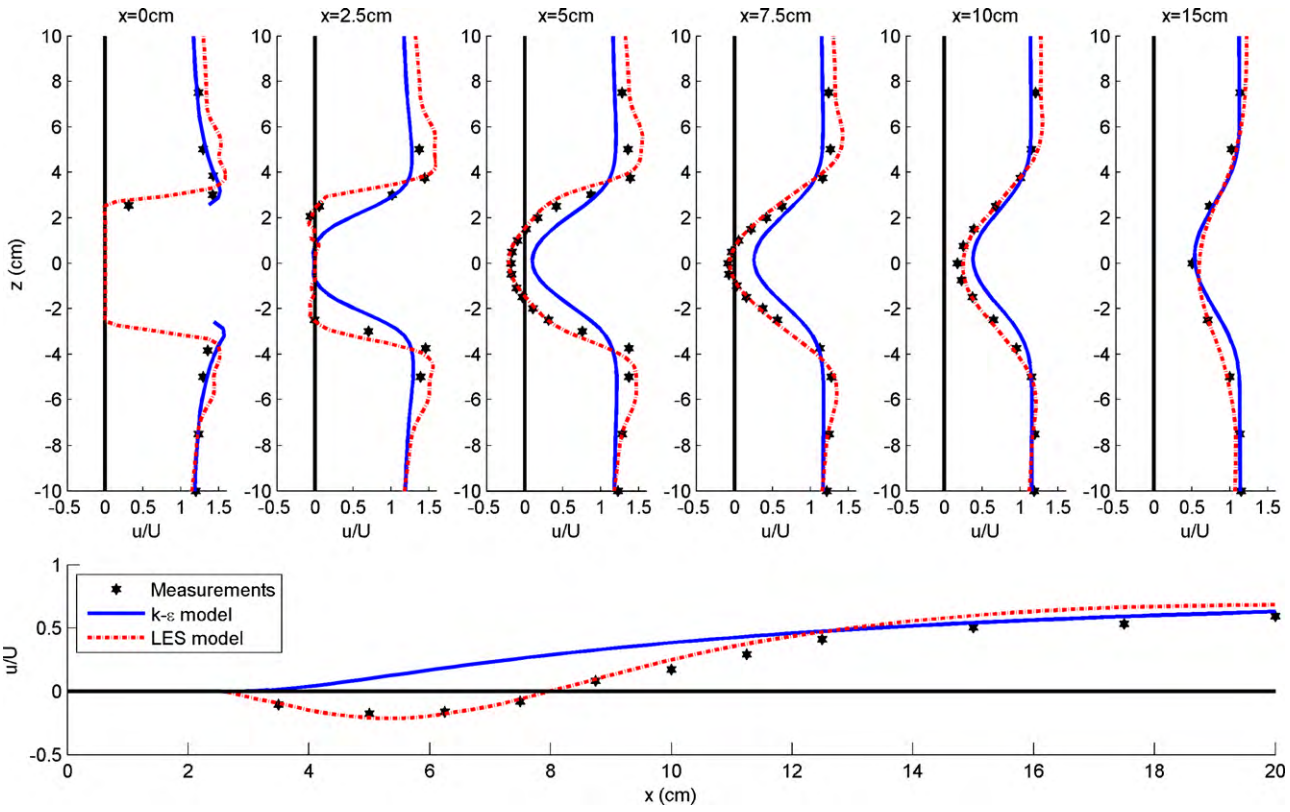

Fig. 1. The flow fields of the CFD models were validated by LDA measurements. The cylinder with a diameter of 5 cm was located at $x = 0$ cm and $z = 0$ cm. The upper panels represent a cross-cut in vertical direction, whereas the lower panel represent a cross-cut in streamwise direction.

ity fields for both models influence the disinfection prediction.

The UV irradiance was calculated by the multiple segment source summation (MSSS) model [14]. For each computational node, the UV irradiance coming from each lamp segment was calculated. Adding up the irradiances for all the segments resulted in the UV irradiance at a particular computational node.

The particles are uniformly injected at the inflow cross-section, where the velocity is also uniformly distributed over the cross-section, so that the ensemble of particles is representative for the fluid volume. The UV dose was recorded for each particle during its path through the reactor. The distribution was obtained by collecting the dose of each particle at the outflow boundary.

The inactivation of microorganisms is modelled by a delayed Chick-Watson model: after a threshold dose, the microorganisms start to be inactivated. The first-order disinfection kinetics describe a linear relation between the log inactivation and the dose. A deviation from this relationship might occur at high inactivation levels, the so-called tailing, which means that no further increase in inactivation is observed at higher UV doses. Since the critical log inactivations occur at lower values, no tailing was considered here. The inactivation of *Bacillus s.* was considered, the kinetic parameters obtained from Hijnen et al. [15] are shown in Table 1.

The flow around a single cross-flow UV lamp was considered to evaluate the different modelling approaches. A UV lamp in a rectangular box was chosen, where the lamp was placed at half of the height. The height and width of the box were both equal to a length of 3 times the cylinder diameter. Four different flow situations were considered: a reference situation and three baffle configurations (Fig. 2):

- Reference, the reference situation with a single UV lamp in a box.
- Baffle upstream, a baffle is placed at the front of the UV lamp (upstream) to force the water elements to flow closer to the lamp.
- Baffle middle, the baffle is placed at the middle of the UV lamp.
- Baffle downstream, the baffle is placed at the rear of the cylinder.

The differences between the baffle configurations are small, but they may have a big impact on the flow field downstream of the lamp. The parameters used for the modelling are shown in Table 1. Normalization is done using the following dose:

$$D_{\text{norm}} = \frac{2P}{Q\alpha}e^{-1}, \tag{1}$$

where P represents the total lamp power in UVC (W), Q is the flow rate (m^3/s) and α is the absorbance (1/m). This characteristic dose value yields a simple estimate for the mean dose that can be expected for a UV system with specific operating conditions [6].

3. Results and discussions

3.1. Mesh independency

For the calculated dose distribution and disinfection, the independency with respect to the grid size, number of particles and

Table 1
Parameters used for the CFD calculations.

Flow rate	Q [m^3/s]	0.005
Baffle height	L [m]	0.025
Total power UVC	P [W]	200
Diameter quartz sleeve	D_{lamp} [m]	0.05
Thickness quartz sleeve	d_q [m]	0.0019
Transmittance water	$T_{10,w}$ [%]	80
Transmittance quartz	$T_{10,q}$ [%]	96
Inactivation constant *Bacillus s.*	k_μ [cm^2/mJ]	0.136
Threshold inactivation *Bacillus s.*	D_0 [mJ/cm^2]	12.3
Normalized dose	D_{norm} [mJ/cm^2]	132

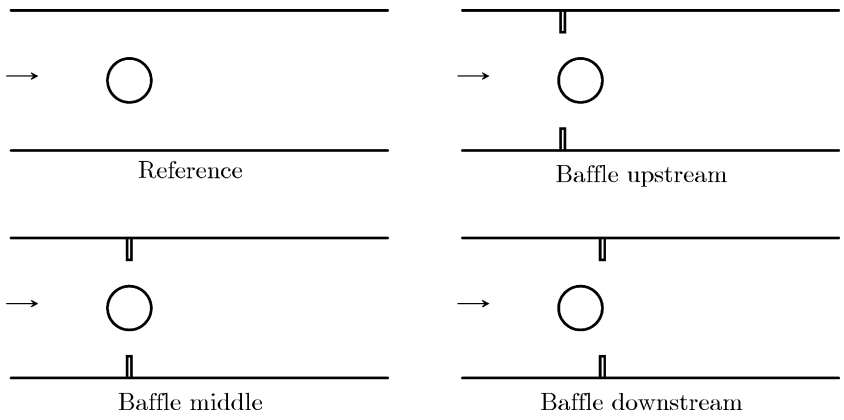

Fig. 2. The flow around a single cylinder was investigated for different baffle configurations.

time stepping of the particle movement was investigated. For the k–ε model, the standard conditions were defined by: a medium grid size (41,228 elements), 4900 particles and a time step of the particle displacement of 0.025 s. These conditions were varied and the dose distribution for each variation is shown in Fig. S2 of the supplementary information. The mean dose (D_{mean}), defined as the average of the doses of all the particles, the minimal dose (D_{min}), defined as the dose of the particle with the lowest dose and disinfection (DE), calculated from the dose of each particle using the delayed Chick-Watson model, are indicated as well. Considering the grid size, a medium grid was sufficient to obtain a converged result for the disinfection (DE). Regarding the number of particles, the dose distribution became smoother by increasing the number of particles. The disinfection results were converged at a number of 10,000 particles, whereas the standard condition of 4,900 particles showed a deviation of 1–2% in comparison with the converged solution. The standard conditions were still used to reduce computational times, allowing a small deviation. The time stepping (Δt) depends on the grid size (Δx) and maximum velocity (u_p), presented by the CFL number ($CFL = u_p\,\Delta t/\Delta x$). For the medium grid size, the solution was converged at a time step of 0.025 s, which corresponds with a maximum CFL number of around 1.

The dependency with respect to the grid size and number of particles is also considered for the LES model (Fig. S3 of the supplementary information). Regarding the time step, the LES model calculated a time-varying velocity field, for which small time steps were needed. These time steps were also used for the particle tracking: they were small enough to obtain a converged solution (CFL number smaller than 1). The standard conditions were: a medium grid size ($64 \times 256 \times 64$) and 50,000 particles. Due to the fluctuations in the velocity field, instead of using a peak release of particles, the particles were injected gradually during the first 1000 time steps to obtain statistically more reliable results. By reducing the mesh size, starting from the coarse grid ($48 \times 192 \times 48$) to the medium grid, the predicted disinfection increased. At the medium grid, the solution was converged; the disinfection at a medium grid size fell within one percent accuracy with respect to the fine mesh ($96 \times 384 \times 96$). This accuracy was regarded as an acceptable choice when trading off the accuracy against computational speed. Regarding the number of particles, the solution was converged at numbers in between 10 000 and 50,000 particles. Both the LES model and the k–ε model use the standard conditions to assess the various UV systems.

3.2. Velocity fields in different configurations

The velocity fields calculated by the k–ε model and LES model are depicted in Figs. 3 and 4, respectively. The streamwise mean velocities (u) are shown for the different flow configurations. In the k–ε model the mean velocity is obtained from the stationary velocity field calculated by the model. In the LES model the mean velocities are obtained by ensemble averaging of the time-varying flow fields. The velocity spatially averaged over the inflow boundary was equal to 0.22 m/s. The water flowed around the cylinder, so that the velocity increased above and below the cylinder, whereas the velocity directly behind the cylinder decreased or even reversed direction due to the obstacle. By placing baffles, the bulk flow was forced to move closer to the lamp. However, the bulk flow had to move through a smaller area, so that the velocity increased even further (up to 4 times the average velocity). Downstream of the baffles large recirculation zones developed. The differences between the k–ε model and LES model were large, especially for the configuration with baffles. For the reference case, differences were noticeable near the wake region. The LES model predicted a distinct region with reversed velocities behind the lamp at a length of around two times the lamp diameter. The k–ε model did not predict reversed velocities, only a reduced velocity downstream of the cylinder which stretched out over a length of a few times the lamp diameter. Also, the LES model showed that the bulk flow moved at a larger distance from the lamp (the wake region was wider). By placing baffles above and below the cylinder, the differences between the models became more apparent. Two jets developed in between the baffles and the cylinder, one above and one below the lamp, which moved differently downstream of the cylinder in both models: The jets predicted by the LES model were more pronounced and stretched over a larger distance, whereas the jets in the k–ε model tended to quickly diffuse over the height. The differences were most pronounced for the configuration with the baffle upstream. The k–ε model predicted no reverse flows downstream of the cylinder here, and the jets had quickly merged. However, in the LES model, the jets did not merge, but moved separately towards the lower and upper wall. Also, a large wake had developed downstream of the lamp. Such a large wake might in fact be unfavorable for the disinfection performance, because the bulk flow did not enter the region with high UV intensities directly behind the lamp. For the configuration with baffles in the middle or downstream, the wakes predicted by the LES model were smaller than for the upstream baffles, because the jets had merged near the centre instead of moving to the outer walls. This shows the sensitivity of the position of the baffles to the flow field: by moving the baffle a little downstream, the direction in which the jets move had changed and the wake was considerable reduced. Small differences might in fact have a large impact on the wake formation. In contrast with the LES model, the size of the wake predicted by the k–ε model was only little influenced by the position of the baffle.

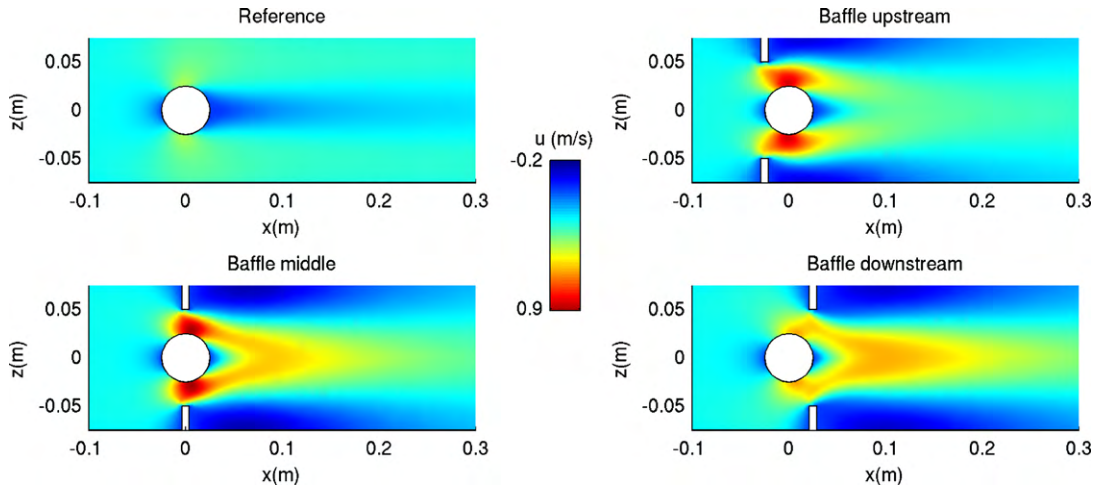

Fig. 3. Velocity field, streamwise velocity u (m/s), calculated by the k–ε model for the different configurations.

Another remarkable result of the LES model was visible for the configuration with a baffle in the middle and a baffle downstream. After the two jets had merged into a single jet, this jet had the tendency to move towards either the upper or lower wall. Due to the symmetry, there is in principal no preference for the upper or lower wall, but once the jet had moved to one side, it remained there. The so-called Coanda effect [16] explains this behaviour: due to small pressure differences the jet is moved towards one side, which increases the pressure difference, eventually resulting in the attachment of the jet to the wall.

3.3. Residence time distribution

The (cumulative) residence time distributions are plotted in Fig. 5. All the particles were instantaneously released in the domain at a distance of 0.15 m upstream of the cylinder. The distribution was obtained by collecting for each particle the time to cover a distance of 0.5 m. The differences between both models became also apparent in the residence time distribution (RTD). Although the differences were still small for the reference case, they clearly marked the differences in underlying velocity fields. In the LES model, the velocity gradients were larger, a higher maximum velocity occurred above and below the cylinder, which resulted in the shortest residence times (T_{10} was shorter). Also, the larger wake region downstream of the cylinder caused the longest residence times (T_{90} was longer). For the configurations with baffles, the differences became more pronounced. The LES model predicted much shorter residence times than the k–ε model. The jets predicted by the LES model were more confined and the recirculation regions were much larger than for the k-ε model. The region of the bulk flow was therefore smaller and, consequently, this region had higher velocities and corresponding lower residence times. The RTD was changed a little by the position of the baffles. The LES model predicted large differences between the baffle configurations, for example the T_{90} was considerably increased by placing the baffle further downstream.

3.4. Dose distribution and disinfection

The UV dose distributions are shown in Fig. 6. The mean dose, minimal dose and disinfection are indicated as well. For the reference case, the differences between the models were small. The peak in the dose distribution was found at the same dose. Since the lower dose part in the distribution was predicted similar for both models, the disinfection predictions were also considered to be equal. The differences were large in the case of the upstream baffle. For the LES model the peak in dose distribution occurred at a similar dose as for the reference situation, whereas for the k–ε model the peak shifted towards a higher dose. As a result, the k–ε model predicted a considerable increase in disinfection (from 1.55 to 2.68 log units)

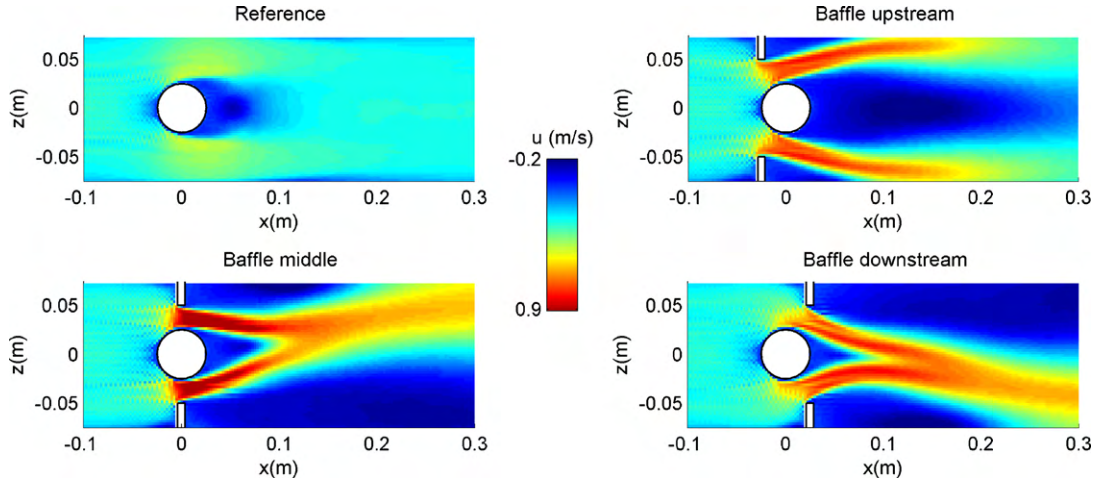

Fig. 4. Velocity field, streamwise velocity u (m/s), calculated by the LES model for the different configurations.

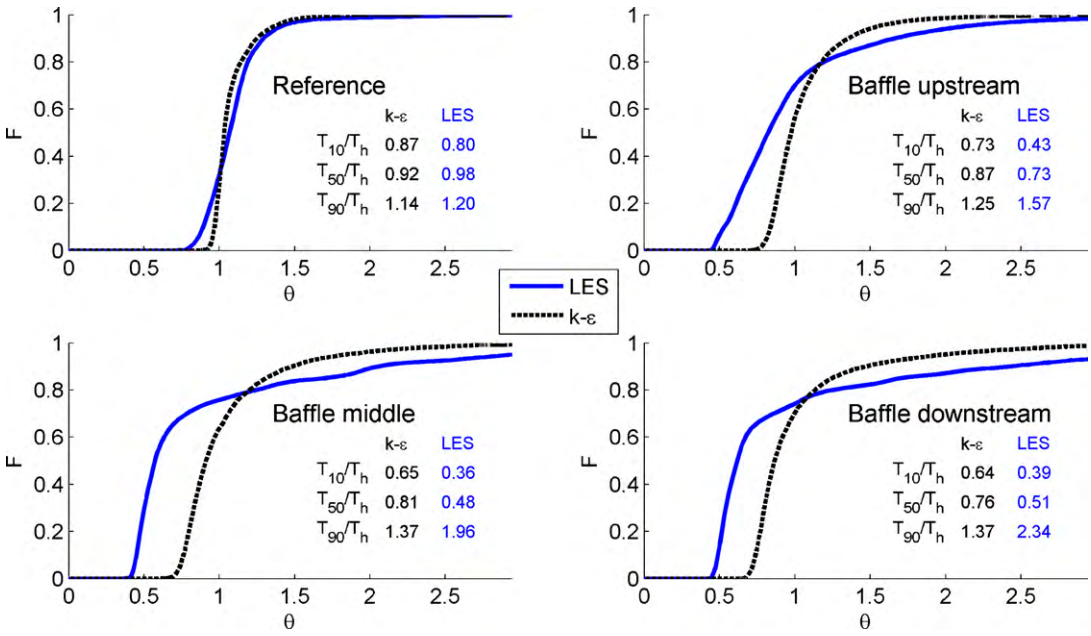

Fig. 5. Cumulative residence time distribution calculated by the k–ε model and LES model for the various geometries ($\theta = t/T_h$).

by placing an upstream baffle, whereas the LES model predicted a decrease in disinfection (from 1.55 to 1.45 log units). The k–ε model showed similar results for the configuration with the baffle in the middle, where the dose distribution closely matched with the upstream baffle configuration. The LES model calculated the peak in the dose distribution at a slightly higher dose than for the reference case, resulting in a small increase in disinfection. However, the peak still occurred at a smaller dose than for the k–ε model, so that the LES model still predicted a smaller disinfection than the k–ε model. By placing the baffle further downstream, the disinfection predicted by the LES model was further increased to 2.11 log units, but not to the extent of the k–ε model prediction (2.49 log units). Here, the differences in dose distribution between the models were smaller than for the other baffle cases, but the LES model still predicted the peak at a lower dose and therefore lower disinfection levels.

The disinfection predictions are summarized in Fig. 7. The predictions were equal for both modelling approaches in the case of the reference situation. Surprisingly, the baffle configurations showed opposite patterns for both models: placing the baffle further downstream resulted in an increase in disinfection for the LES model, whereas the k–ε model predicted a decrease in disinfection. The best results for the k–ε model were obtained for the upstream baffle, where the LES model predicted the worst disinfection results. This increase in disinfection for the LES model can be explained by the size of the wake: moving the baffles downstream reduced the wake, so that the bulk flow moved through an area with higher UV intensities, resulting in higher UV doses.

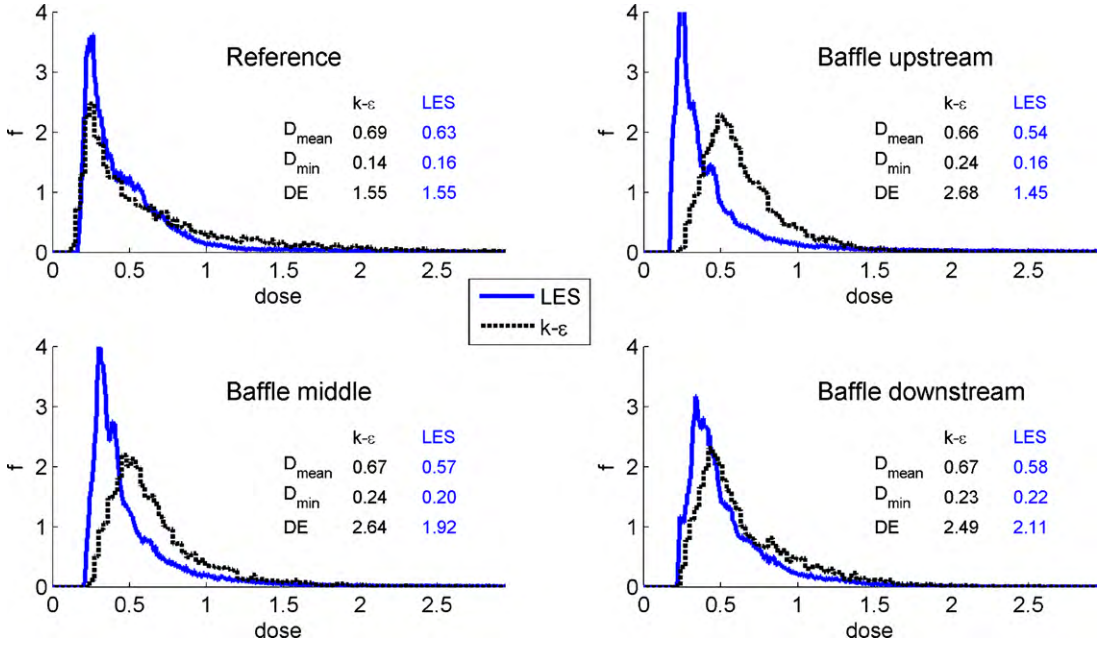

Fig. 6. UV dose distributions calculated by the k–ε model and LES model for the various geometries. The dose is scaled with a characteristic dose D_{scale}. Disinfection (DE), minimal dose and mean dose are indicated as well.

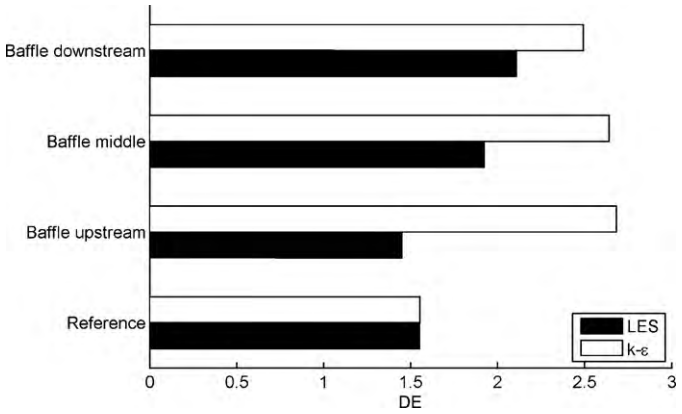

Fig. 7. Overview of the disinfection levels, predicted by the LES model and k–ε model for the various geometries.

The differences between the modelling approaches become more apparent by considering the movements of the individual particles (Figs. 8 and 9). The particles are released by means of a pulse injection upstream of the UV lamp. The turbulent eddies that are resolved in the LES model cause a more discontinuous particle distribution, resulting in areas with high concentration of particles and areas without particles (white areas). Since the k–ε model uses an isotropic turbulent viscosity coefficient to mimic the turbulent eddies, the particle distribution is smoother. For the reference case, we have seen from earlier observations that the LES model predicted smaller residence times than the k–ε model, whereas the peak in the dose distribution occurred at a similar dose. These observations can be related to the particles positions and the UV dose received by the particle. Clearly, the way the particles had moved was different for both models. The k–ε model predicted a more smooth concentration distribution of particles due to the smaller velocity gradients and small wake region. The region downstream of the lamp was therefore quickly filled with particles. From the particle positions calculated by the LES model, the turbulent flow features were better recognizable. For example, in the case of the reference cylinder at $t/T_h = 0.25$ in Fig. 8, the large wake was visible by the particles that moved around it. An instant later, the large eddies shed from the cylinder were visible: they caused mixing of low and high dose particles. Subsequently, particles were trapped inside the wake region, where they received very high doses. The LES model predicted the quickest moving particles due to the higher maximum velocities, which occurred at a small distance above as well as below the lamp. These particles did not necessarily have the smallest dose. In fact, these particles moved close to the lamps, where the irradiances were high. Instead, the particles with the lowest doses had moved along the upper and lower wall. After they had passed the lamp, they were – after a while – redistributed over the height due the increased turbulent mixing downstream of the lamp. Since the velocity fields near the outer walls were almost similar for both models, the critical particles, which are the particles with the lowest doses, were predicted the same. As a result, the disinfection prediction for the reference case was equal for both models.

Next, the particle positions for the baffle upstream configuration are considered in Fig. 9. For this configuration, the differences in disinfection levels predicted by both models were large. The criti-

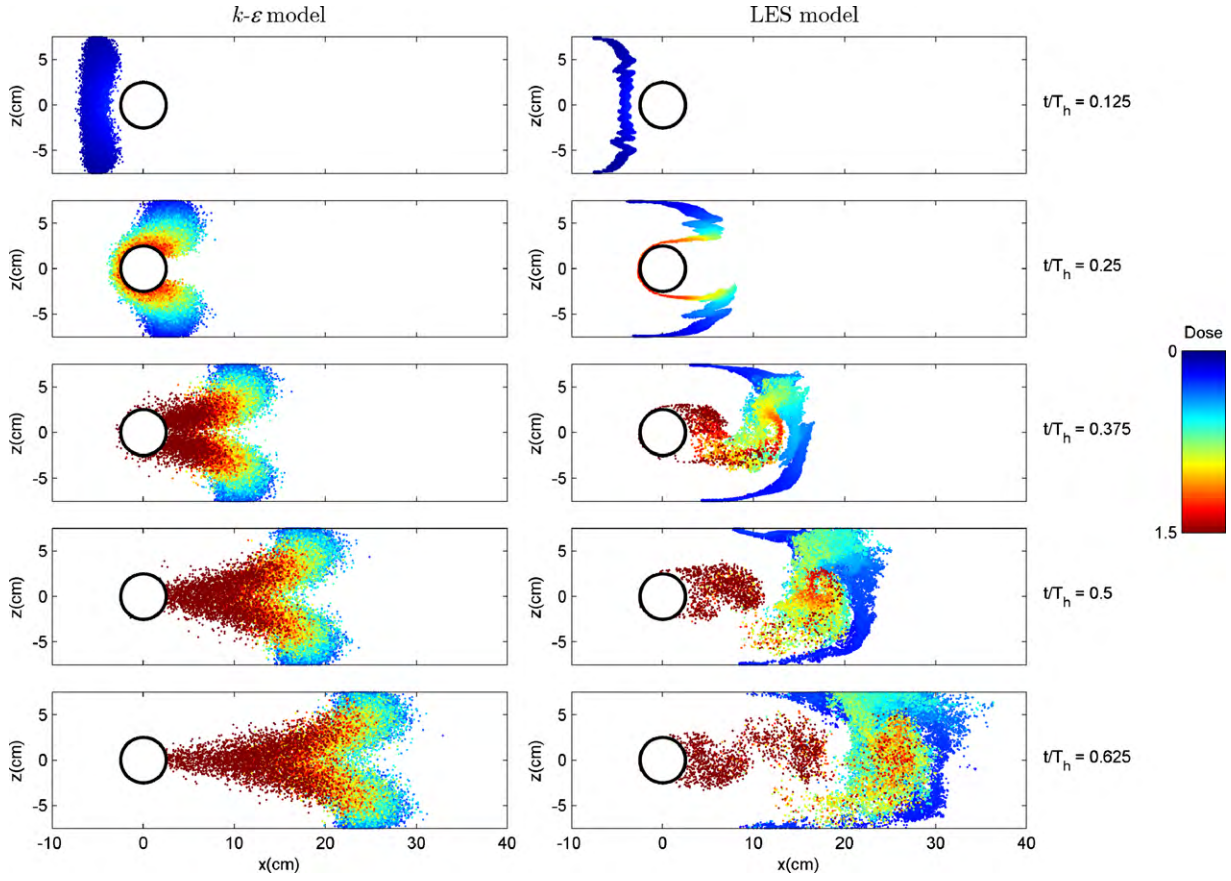

Fig. 8. Particle positions calculated by the k–ε model (left panel) and LES model (right panel) after a peak release of particles upstream at different time steps for the reference cylinder. The scaled dose is indicated by the color of the particle. The initial stages after particle release are shown, which represent the low dose particles that are most important for disinfection.

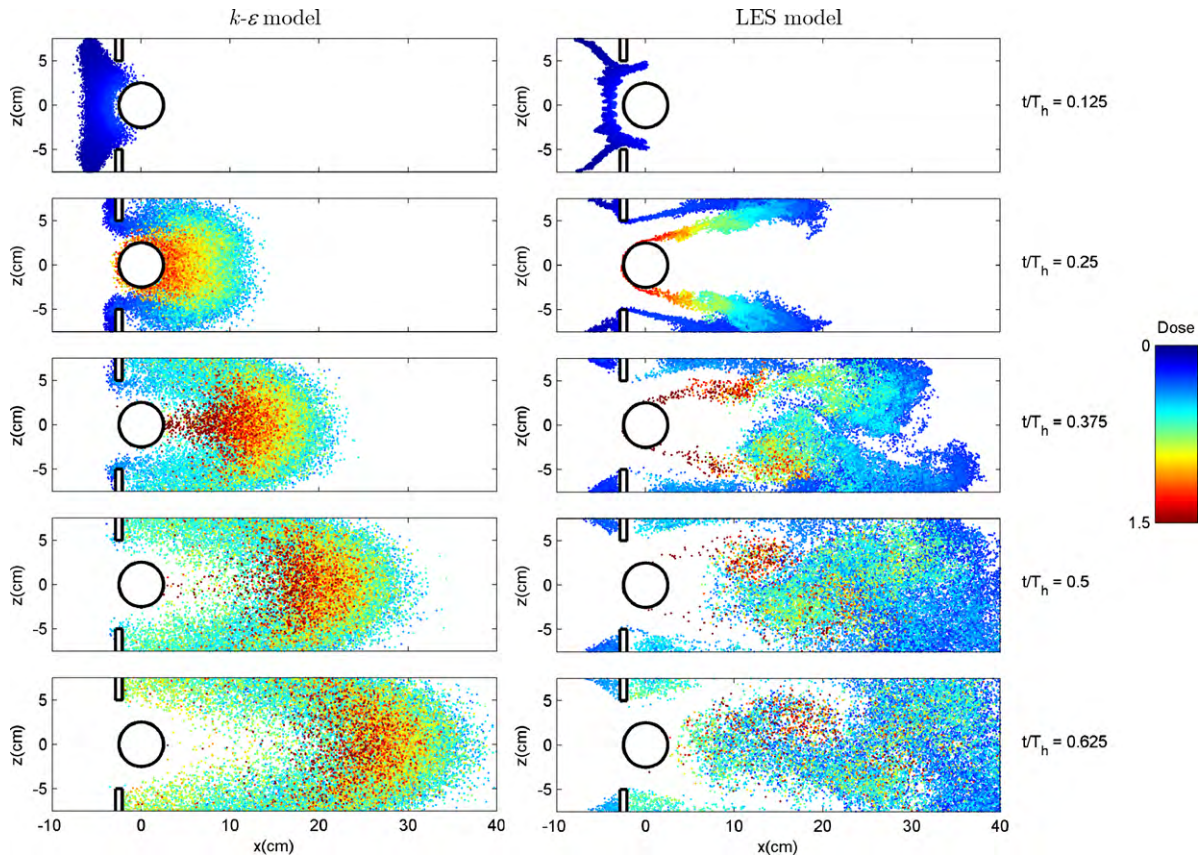

Fig. 9. Particle positions calculated by the k–ε model (left panel) and LES model (right panel) after a peak release of particles upstream at different time steps for the upstream baffle. The scaled dose is indicated by the color of the particle. The initial stages after particle release are shown, which represent the low dose particles that are most important for disinfection.

cal flow trajectories from the reference configuration—the particles with the lowest doses moving along the outer walls, were forced to move around the baffle. The differences between the models is most clearly observed at $t/T_h = 0.25$. The k–ε model predicted a spreading of particles over the height, including a large group of particles directly downstream of the lamp, whereas the LES model predicted particles close to the outer walls, which had moved along with the jets above and below the lamp. Due to the high velocities here, the UV doses remained small. Further downstream, these particles were redistributed over the height, but at such a distance from the lamp that the doses remained small. Therefore, at $t/T_h = 0.375$, the LES model predicted large numbers of particles close to the outflow, which were responsible for the low residence times and low doses. For the k–ε model, the particles had moved slower and closer to the lamps, so that the peak in the dose distribution occurred at a higher dose. Consequently, the predicted disinfection levels differed largely. The longer tail in the RTD predicted by the LES model was caused by the large wake region, which is visible by the particles trapped inside this region. These particles are still moving in reverse direction (towards the lamp), and will receive higher doses when they come closer to the lamp at $t/T_h > 0.625$.

3.5. Conclusions

UV systems often contain a number of lamps placed perpendicular to the flow direction. Predicting the flow fields around these lamps requires sophisticated modelling of the turbulent flow features. CFD models that use a RANS approach, such as the standard k–ε model, have difficulties with these flow configurations. This modelling approach does not capture the complex turbulent motions in detail, which leads to inaccuracies in the flow field prediction, clearly observed by the under prediction of the wake region behind the lamp. Using more advanced modelling techniques, such as a large-eddy simulation, which resolves more details of the turbulent flow, the flow fields in the wake region are predicted more precisely. Both modelling techniques were compared to velocity measurements of the flow around a single cylinder. The wake region was indeed largely under predicted by the k–ε model, whereas the LES model resembled the measurements well.

Using both modelling approaches, the sensitivity of the residence time distribution, dose distribution and disinfection to the local velocity field was investigated. This approach clarifies the importance of predicting local flow features, such as wakes, precisely. Four configurations were considered: a reference situation with one cylinder placed perpendicular to the flow direction. In addition, baffles placed at different positions (upstream, in the middle and downstream of the lamp) were added. The flow around a cylinder is known to be very sensitive to the local flow situation, the turbulent flow influences the boundary layer at the cylinder surface, as well as the size of the wake. By placing baffles above and below the cylinder the situation becomes even more complicated: recirculations develop downstream of the baffles, turbulent eddies are shed from the baffles and a mixing layer develops. All these flow features influence the flow around and downstream of the cylinder. The flow fields were therefore predicted differently for both modelling approaches; some small differences with respect to the wake size were observed for the reference situation, which became more pronounced by placing baffles. In the case of a baffle upstream of the cylinder, the differences were the largest. The k–ε model predicted a small wake, whereas the LES model predicted a

very large wake. The residence time distribution and dose distribution also showed marked differences. The disinfection prediction was the same for both models in the case of the reference cylinder. Here, the part with the lowest doses in the dose distribution was similar, which is related to the particles that had moved close to the outer walls. This region was not influenced by the wake and showed similar velocity profiles for both models. By placing baffles the differences in disinfection prediction became large, especially for the upstream baffle, where the k–ε model predicted a significant higher disinfection than the LES model.

The weaknesses of RANS models, that do not resolve the turbulent motions, were demonstrated. By simplifying the turbulent flow inside the UV system, flow fields are predicted inaccurately in time and space. How much this affects the disinfection prediction depends on the local geometry. As shown here for the baffle configurations, the predictions of the k–ε model became inaccurate in situations where large velocity differences are present and large wakes can develop. The latter might not be the case for full-scale installations, where the wakes are more confined due the interaction with other lamps. Nevertheless, when using these types of models one must be aware of the limitations of the turbulence models. More advanced models, such as the LES model, will result in a more precise disinfection prediction, but are computationally more expensive.

Acknowledgements

This work was performed partly in the TTIW-cooperation framework of Wetsus, centre of excellence for sustainable water technology (www.wetsus.nl). Wetsus is funded by the Dutch Ministry of Economic Affairs. The authors like to thank the participants of the research theme clean water technology for the fruitful discussions and their financial support.

Appendix A. Supplementary data

Supplementary data associated with this article can be found, in the online version, at doi:10.1016/j.cej.2010.05.055.

References

[1] E.R. Blatchley III, Z. Do-Quang, M.L. Janex, J.M. Laine, Process modeling of ultraviolet disinfection, Water Sci. Technol. 38 (1998) 63–69.
[2] D.A. Lyn, K. Chiu, E.R. Blatchley, Numerical modeling of flow and disinfection in UV disinfection channels, J. Environ. Eng. 125 (1999) 17–26.
[3] K. Chiu, D.A. Lyn, P. Savoye, E.R. Blatchley, Effect of UV system modifications on disinfection performance, J. Environ. Eng. 125 (1999) 459–469.
[4] J. Ducoste, K. Linden, D. Rokjer, D. Liu, Assessment of reduction equivalent fluence bias using computational fluid dynamics, Environ. Eng. Sci. 22 (2005) 615–628.
[5] D.A. Sozzi, F. Taghipour, UV reactor performance modeling by Eulerian and Lagrangian methods, Environ. Sci. Technol. 40 (2006) 1609–1615.
[6] B.A. Wols, J.A.M.H. Hofman, E.F. Beerendonk, W.S.J. Uijttewaal, J.C. Van Dijk, Design of hydraulically optimized UV systems using CFD, in: IUVA—5th UV World Congress, Amsterdam, 2009.
[7] M. Breuer, A challenging test case for large eddy simulation: high Reynolds number circular cylinder flow, Int. J. Heat Fluid Flow 21 (2000) 648–654.
[8] B.A. Wols, W.S.J. Uijttewaal, L.C. Rietveld, J.A.M.H. Hofman, J.C. Van Dijk, Hydraulic optimization of a single UV lamp placed perpendicular to the flow direction by experimental and numerical techniques, in: IO3A 19th World Congress & Exhibition, Tokyo, Japan, 2009.
[9] D. Liu, C. Wu, K. Linden, J. Ducoste, Numerical simulation of UV disinfection reactors: evaluation of alternative turbulence models, Appl. Math. Modell. 31 (2007) 1753–1769.
[10] D.A. Lyn, E.R.I. Blatchey, Numerical computational fluid dynamics-based models of ultraviolet disinfection channels, J. Environ. Eng. 131 (2005) 838–849.
[11] A. Munoz, S. Craik, S. Kresta, Computational fluid dynamics for predicting performance of ultraviolet disinfection—sensitivity to particle tracking inputs, J. Environ. Eng. Sci. 6 (2007) 285–301.
[12] C. Moeng, A large-eddy-simulation model for the study of planetary boundary-layer turbulence, J. Atmos. Sci. 41 (1984) 2052–2062.
[13] W. van Balen, W.S.J. Uijttewaal, K. Blanckaert, Large-eddy simulation of a mildly curved open-channel flow, J. Fluid Mech. 630 (2009) 413–442.
[14] D. Liu, J.J. Ducoste, S. Jin, K. Linden, Evaluation of alternative fluence rate distribution models, J. Water Supply Res. Technol. Aqua 53 (2004) 391–408.
[15] W.A.M. Hijnen, E.F. Beerendonk, G.J. Medema, Inactivation credit of UV radiation for viruses, bacteria and protozoan (oo)cysts in water: a review, Water Res. 40 (2006) 3–22.
[16] R. Wille, H. Fernholz, Report on the first European mechanics colloquium, on the Coanda effect, J. Fluid Mech. 23 (1965) 801–819.
[18] J. Baldyga, W. Orciuch, Barium sulphate precipitation in a pipe—an experimental study and CFD modeling, Chem. Eng. Sci. 56 (2001) 2435–2444.
[19] G.J.M. Uffink, Analysis of Dispersion by the Random Walk Method, PhD Thesis, Delft University of Technology, 1990.
[20] B.A. Wols, L. Shao, W.S.J. Uijttewaal, J.A.M.H. Hofman, L.C. Rietveld, J.C. van Dijk, Evaluation of experimental techniques to validate numerical computations of the hydraulics inside a UV bench-scale reactor, Chem. Eng. Sci. 65 (2010) 4491–4502.